

Supplementary Information

A fine-tuned fluorinated MOF addresses the needs for trace CO₂ removal and air capture using physisorption

Prashant M. Bhatt,[†] Youssef Belmabkhout,[†] Amandine Cadiou,[†] Karim Adil,[†] Osama Shekhah,[†] Aleksander Shkurenko,[†] Leonard J. Barbour[‡] and Mohamed Eddaoudi^{*,†}

[†]Functional Materials Design, Discovery & Development Research Group (FMD³), Advanced Membranes & Porous Materials Center, Division of Physical Sciences and Engineering, King Abdullah University of Science and Technology (KAUST), Thuwal 23955-6900, Kingdom of Saudi Arabia, E-mail: mohamed.eddaoudi@kaust.edu.sa

[‡]Department of Chemistry and Polymer Science, University of Stellenbosch, Stellenbosch 7600, South Africa

Table of contents

1. Single crystal X-ray structure data	S2
2. Powder X-ray diffraction patterns	S4
3. Variable temperature powder X-ray diffraction patterns	S5
4. Variable humidity powder X-ray diffraction patterns	S6
5. TGA plot for NbOFFIVE -1-Ni	S7
6. Gas adsorption experiments	S8
7. Breakthrough experiments	S11
8. TG-DSC experiments	S14
9. References	S15

1. Single crystal X-ray structure data

Single Crystal X-ray Diffraction data were collected on a Bruker X8 PROSPECTOR APEX2 CCD diffractometer using Cu $K\alpha$ radiation ($\lambda = 1.54178 \text{ \AA}$). Indexing was performed using APEX2 (Difference Vectors method).¹ Data integration and reduction were performed using SaintPlus 8.34.² Absorption correction was performed by multi-scan method implemented in SADABS.³ Space group was determined using XPREP implemented in APEX2. Structure was solved using Direct Methods (SHELXS-97) and refined using SHELXL-97 (full-matrix least squares on F^2) contained WinGX v1.70.01.⁴

Table S1. Single crystal X-ray structure data and refinement conditions for $\text{NiNbOF}_5(\text{pyr})_2 \cdot 2\text{H}_2\text{O}$ (**1**).

Empirical formula	$\text{C}_8\text{H}_{12}\text{F}_5\text{N}_4\text{NbNiO}_3$
Formula weight	458.84
Crystal system, space group	Tetragonal, $I4/mcm$
Unit cell dimensions	$a = 9.942(4) \text{ \AA}$, $c = 15.764(6) \text{ \AA}$
Volume	$1558(1) \text{ \AA}^3$
Z, calculated density	4, 1.956 Mg m^{-3}
$F(000)$	904
Temperature (K)	295.5(1)
Radiation type, λ	Mo $K\alpha$, 0.71073 \AA
Absorption coefficient	2.01 mm^{-1}
Absorption correction	Multi-scan
Max and min transmission	0.745 and 0.0483
Crystal size	$0.03 \times 0.04 \times 0.04 \text{ mm}$
θ range for data collection	$2.6\text{--}25.0^\circ$
Limiting indices	$-10 \leq h \leq 11$, $-11 \leq k \leq 11$, $-15 \leq l \leq 18$
Reflection collected / unique / observed with $I > 2\sigma(I)$	3163 / 396 ($R_{\text{int}} = 0.095$) / 225
Completeness to $\theta_{\text{max}} = 25.0^\circ$	100.0 %
Refinement method	Full-matrix least-squares on F^2
Data / restraints / parameters	396 / 0 / 34
Final R indices [$I > 2\sigma(I)$]	$R_1 = 0.033$, $wR_2 = 0.068$
Final R indices (all data)	$R_1 = 0.070$, $wR_2 = 0.077$
Weighting scheme	$[\sigma^2(F_o^2) + (0.0377P)^2]^{-1*}$
Goodness-of-fit	0.98
Largest diff. peak and hole	0.67 and -0.62 e \AA^{-3}

* $P = (F_o^2 + 2F_c^2)/3$

Table S2. Single crystal X-ray structure data and refinement conditions for NiNbOF₅(pyr)₂·0.84(CO₂) (**2**).

Empirical formula	C _{8.84} H ₈ F ₅ N ₄ NbNiO _{2.68}
Formula weight	459.81 g/mol
Crystal system, space group	Tetragonal, <i>I4/mcm</i>
Unit cell dimensions	<i>a</i> = 9.903(1) Å, <i>c</i> = 15.720(2) Å
Volume	1541.6(4) Å ³
<i>Z</i> , calculated density	4, 1.981 g cm ⁻³
<i>F</i> (000)	898
Temperature (K)	296(1)
Radiation type, λ	Cu <i>K</i> α , 1.54178 Å
Absorption coefficient	8.27 mm ⁻¹
Absorption correction	Multi-scan
Max and min transmission	0.584 and 0.350
Crystal size	0.01 × 0.02 × 0.03 mm
θ range for data collection	5.6–66.9°
Limiting indices	-11 ≤ <i>h</i> ≤ 11, -11 ≤ <i>k</i> ≤ 11, -18 ≤ <i>l</i> ≤ 18
Reflection collected / unique / observed with <i>I</i> > 2σ(<i>I</i>)	13098 / 392 (<i>R</i> _{int} = 0.070) / 295
Completeness to θ_{max} = 66.9°	99.0 %
Refinement method	Full-matrix least-squares on <i>F</i> ²
Data / restraints / parameters	392 / 13 / 40
Final <i>R</i> indices [<i>I</i> > 2σ(<i>I</i>)]	<i>R</i> ₁ = 0.071, <i>wR</i> ₂ = 0.184
Final <i>R</i> indices (all data)	<i>R</i> ₁ = 0.078, <i>wR</i> ₂ = 0.189
Weighting scheme	[σ ² (<i>F</i> _o ²) + (0.0906 <i>P</i>) ² + 19.1958 <i>P</i>] ⁻¹ *
Goodness-of-fit	1.04
Largest diff. peak and hole	1.44 and -0.52 e Å ⁻³

* $P = (F_o^2 + 2F_c^2)/3$

2. Powder X-ray diffraction patterns

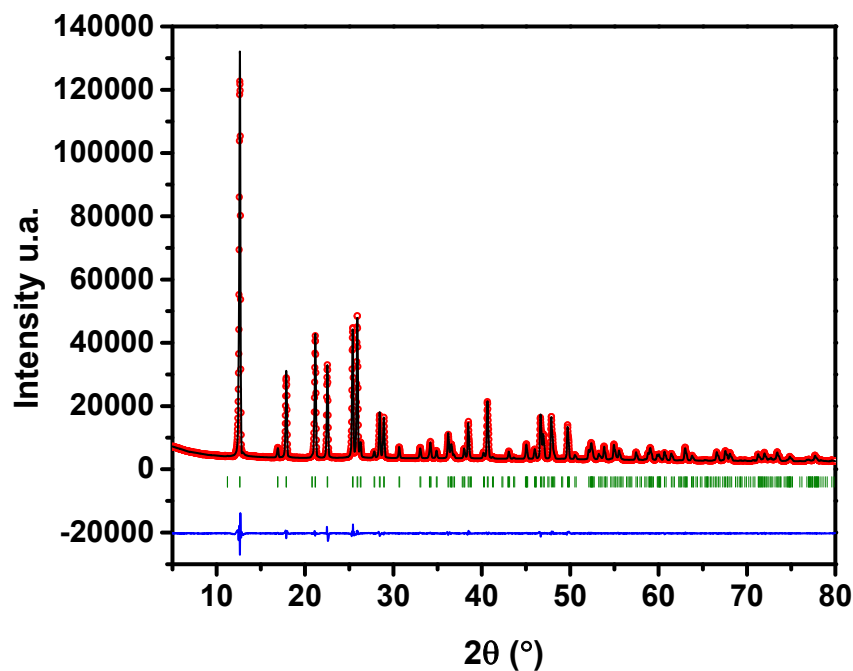


Figure S1. Final Le Bail profile refinement⁵ with observed (black line), calculated (red point), and difference (blue line) profiles of X-ray diffraction data, vertical green bars are related to the calculated Bragg reflection positions, of **NbOFFIVE-1-Ni** ($R_p = 0.074$, $R_{wp} = 0.079$, $R_{exp} = 0.031$, $\chi^2 = 6.73$).

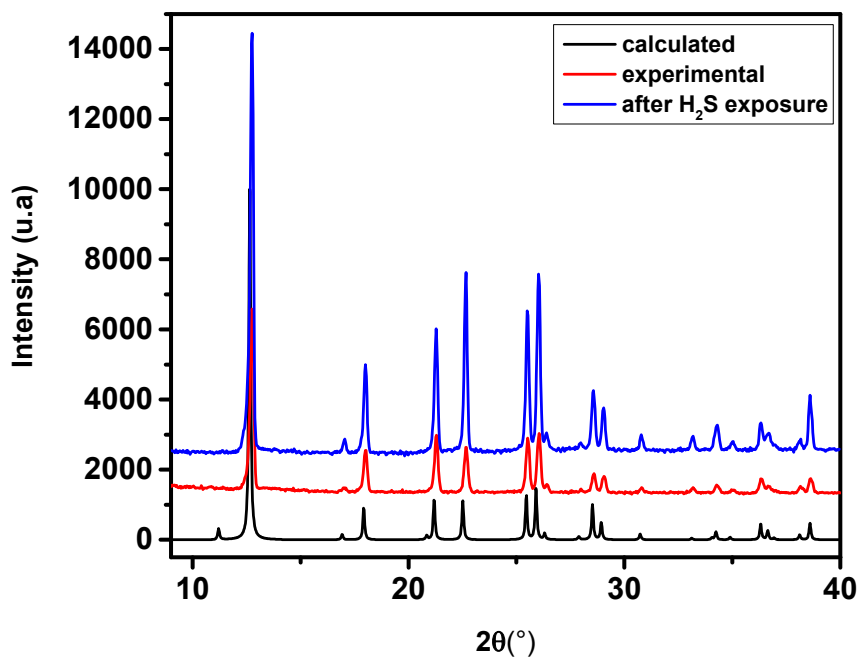


Figure S2. Powder X-ray diffraction (PXRD) patterns calculated from single crystal X-ray structure data (black), experimental (red) and after H_2S exposure (blue) of **NbOFFIVE-1-Ni**.

3. Variable temperature powder X-ray diffraction Patterns

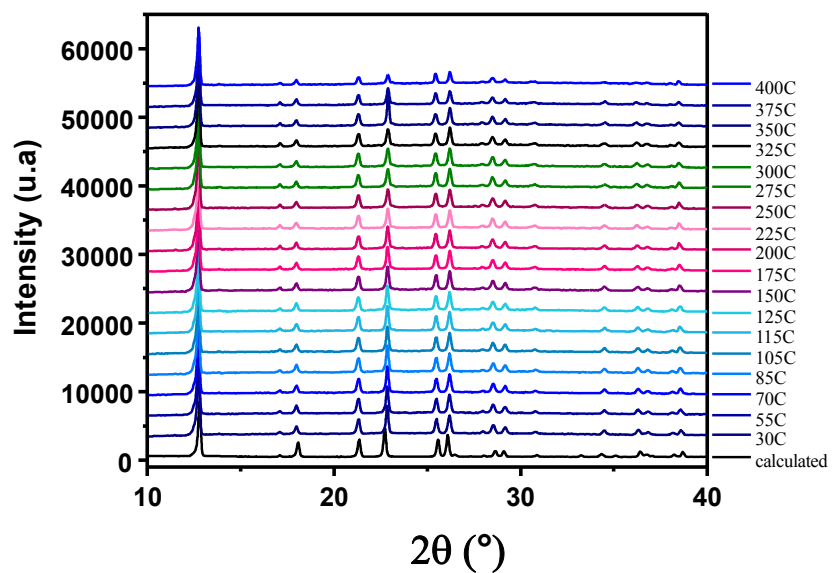


Figure S3. Calculated and experimental powder X-ray diffraction (PXRD) patterns for **NbOFFIVE-1-Ni** recorded at variable temperatures.

4. Variable humidity powder X-ray diffraction patterns

Comparison of the PXRD patterns confirms that no phase transition appears over this humidity range and the framework of **NbOFFIVE**-1-Ni remains intact.

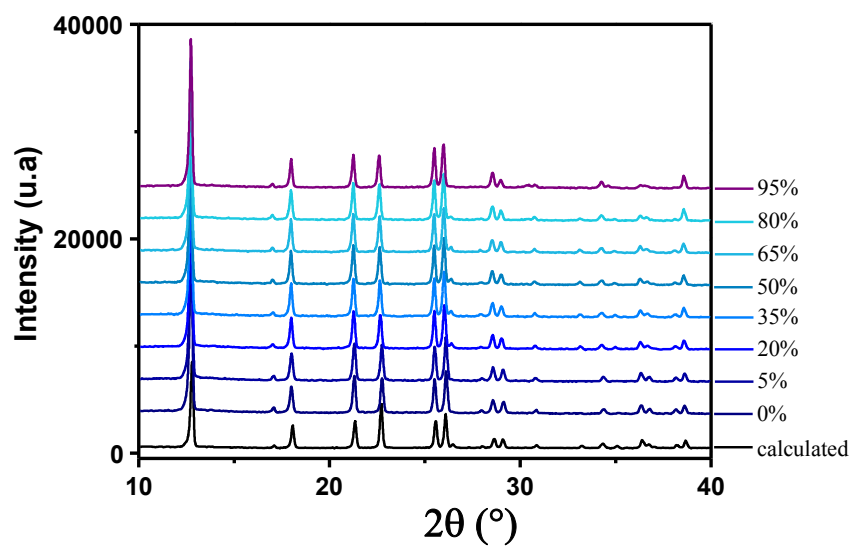


Figure S4. Calculated and experimental powder X-ray diffraction (PXRD) patterns for **NbOFFIVE**-1-Ni recorded at variable humidity levels.

5. TGA plot for NbOFFIVE-1-Ni

TGA plot shows that the as-synthesized sample loses water between 30 °C and 150 °C followed by a plateau from 150-280 °C. The weight loss of 8% between 20 °C and 280 °C corresponds to a loss of two water molecules (calc. 7.8 wt%). Noticeably, the material decomposition starts above 300 °C.

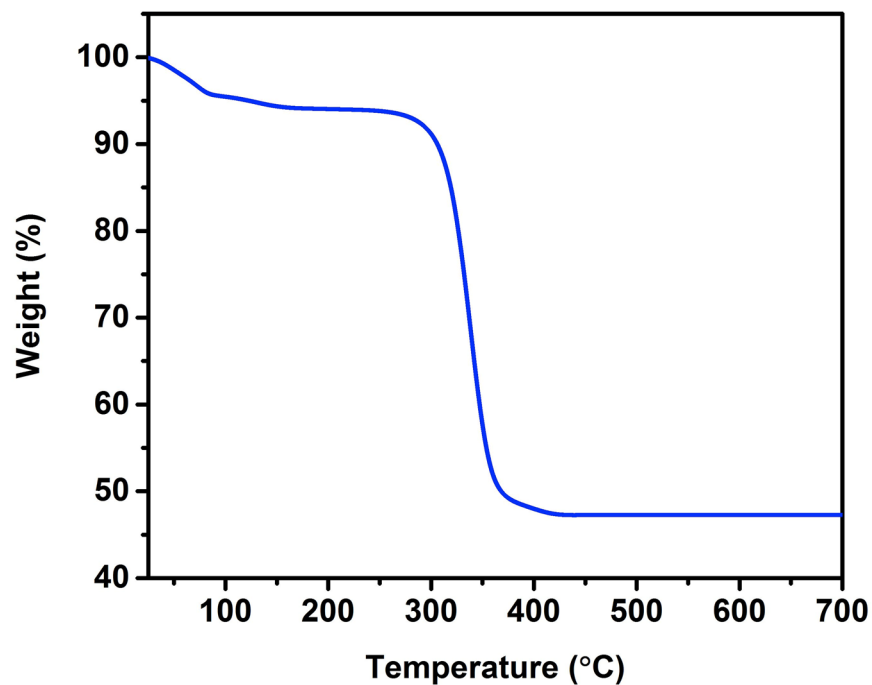
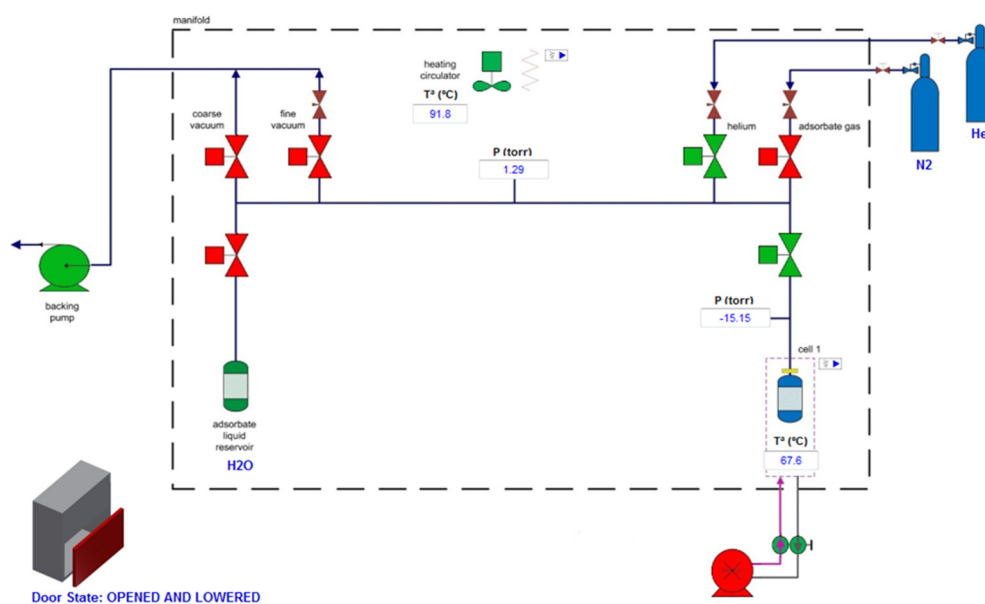


Figure S5. TGA plot of the as synthesized **NbOFFIVE-1-Ni** under N₂ flux with a heating rate of a 5 °C per minute.

6. Gas adsorption experiments

Vstar¹ vapor sorption analyzer from Quantachrome instruments was used for water sorption (Scheme S1). In a typical experiment, sample was activated in-situ at 105 °C under dynamic vacuum for 8 hours. Temperature was increased to 105 °C from room temperature at the rate of 1 °C/min. Activated sample was used for corresponding isotherm measurement. All the sorption experiments were carried out at 25 °C sample temperature unless otherwise mentioned. Manifold temperature was maintained at 90 °C throughout the measurement. Sorption data were processed by using Helmholtz equation.



Scheme S1. Schematic diagram of Vstar1 vapor sorption analyzer.

Low-pressure gas sorption measurements were performed on a fully automated Quadrasorb SI (for CO₂ sorption screening) and Autosorb-iQ gas adsorption analyzer, (Quantachrome Instruments) at relative pressures up to 1 atm. The bath temperature for the CO₂ sorption measurements was controlled using an ethylene glycol/H₂O re-circulating bath.

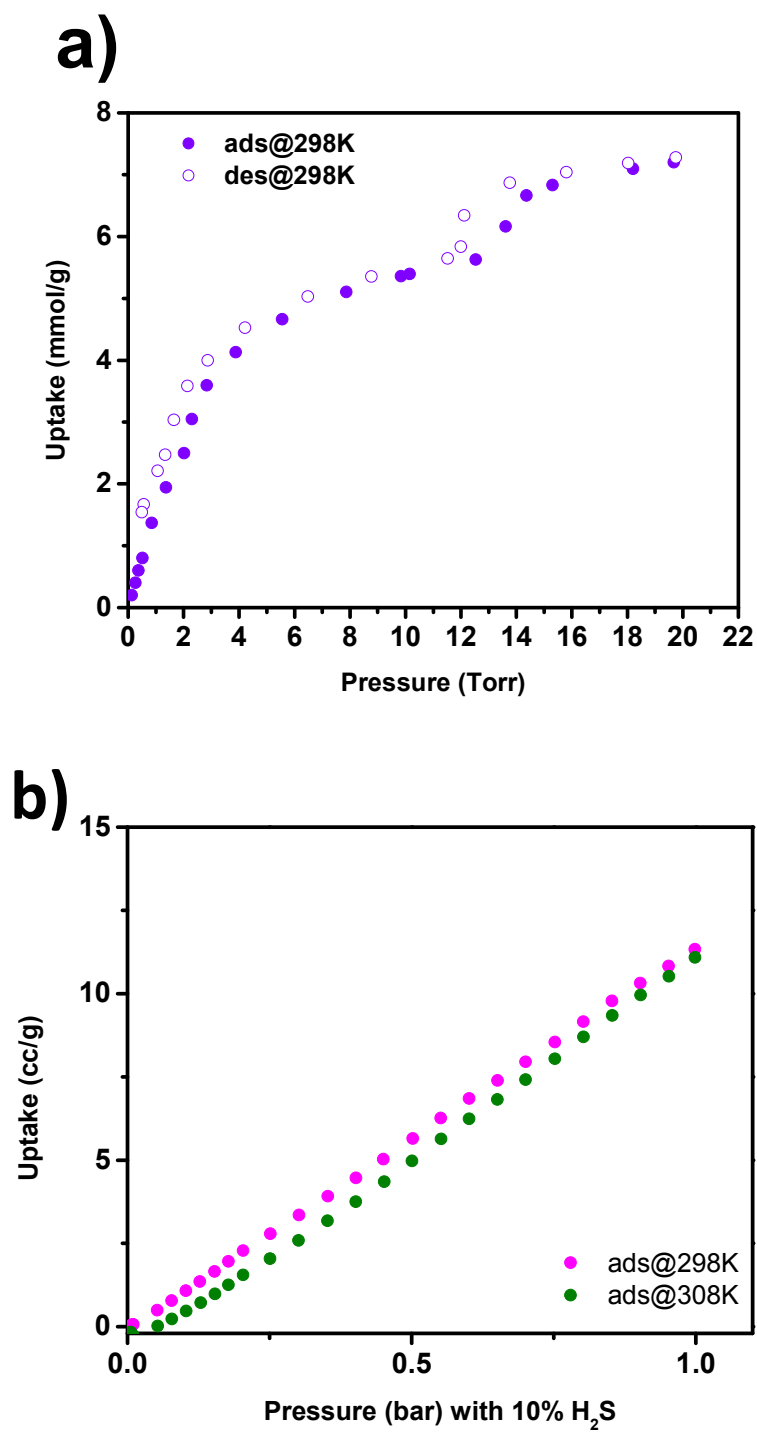


Figure S6. a) H₂O sorption isotherms at 298 K of NbOFFIVE-1-Ni, b) H₂S sorption isotherms at 298 and 308 K of NbOFFIVE-1-Ni.

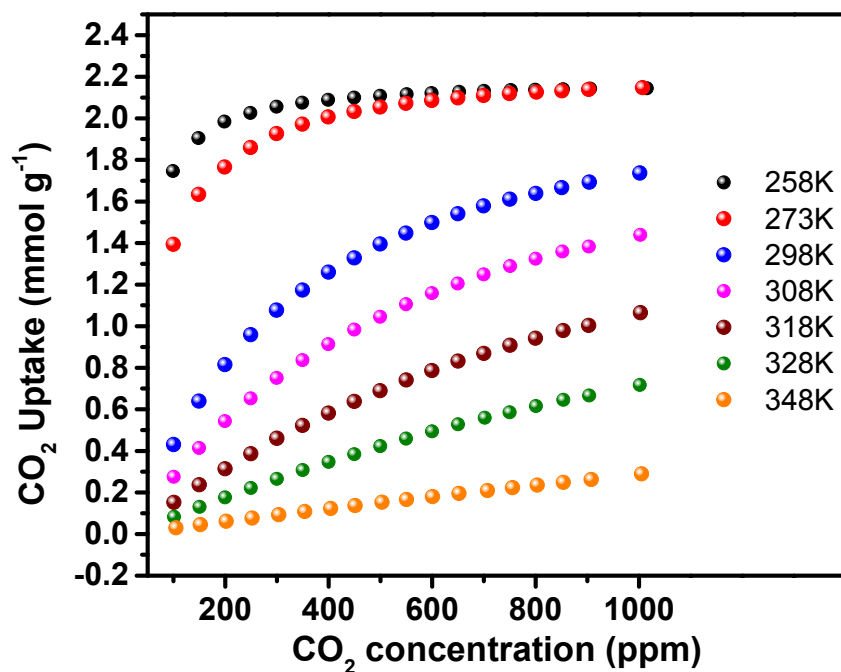


Figure S7. CO₂ sorption isotherms at 258, 273, 298, 308 and 318 K of **NbOFFIVE-1-Ni** up to 1000 ppm CO₂ concentration.

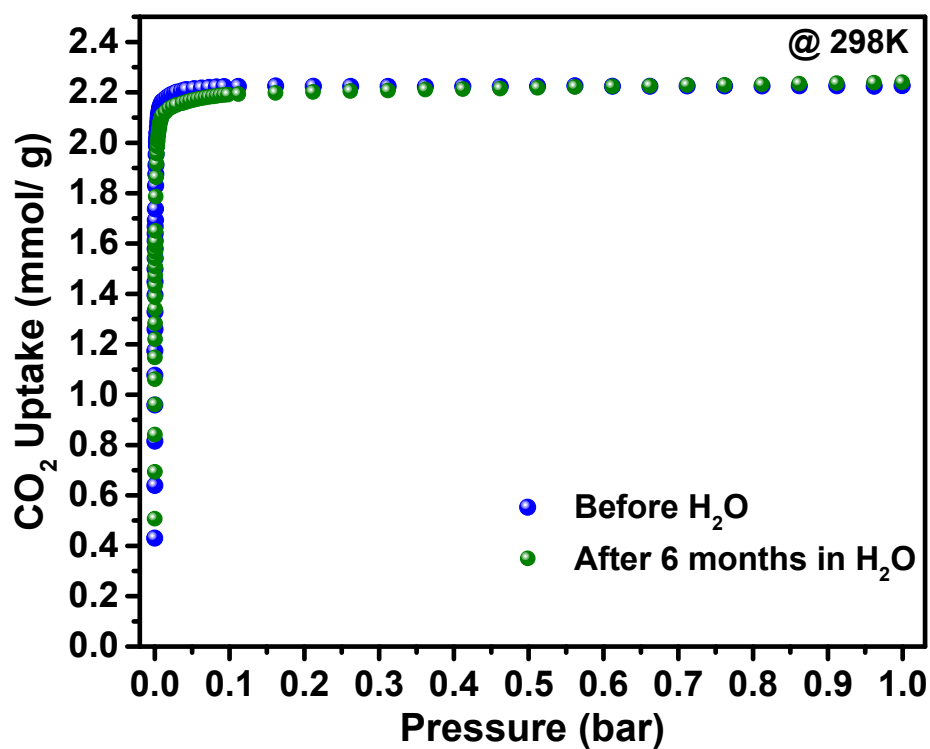
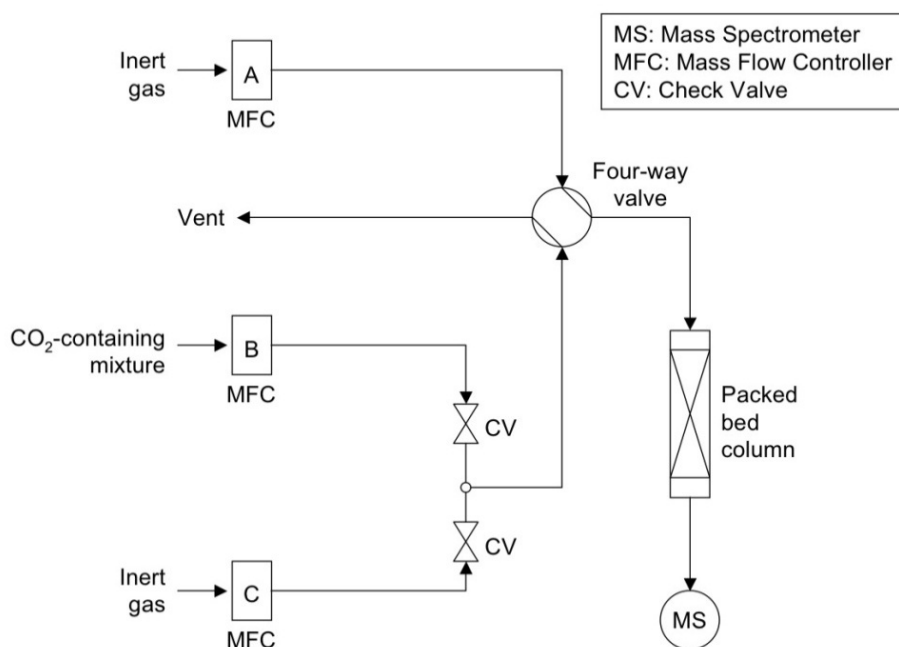


Figure S8. The CO₂ adsorption isotherms for **NbOFFIVE-1-Ni** at 298 K, collected before and after the material immersion for six months in water.

7. Breakthrough experiments

The experimental set-up used for dynamic breakthrough measurements is shown in Scheme S2. The gas manifold consisted of three lines fitted with mass flow controllers Line “A” is used to feed an inert gas, most commonly helium, to activate the sample before each experiment. The other two lines, “B” and “C” feed a pure or pre-mixed gases. Whenever required, gases flowing through lines “B” and “C” may be mixed before entering a column packed with **NbOFFIVE**-1-Ni using a four-way valve. In a typical experiment, 1g of adsorbent (in the column) was activated at 378 K overnight under vacuum in a separate oven.

After the sample is degassed, the column is backfilled with argon and mounted in the set-up. Before starting each experiment, helium reference gas is flushed through the column and then the gas flow is switched to the desired gas mixture at the same flow rate of 10 cm³/g (20 cm³/g in case of 1000 ppm CO₂). The gas mixture downstream the column was monitored using a Hiden mass-spectrometer.



Scheme S2. Representation of the column breakthrough experiment.

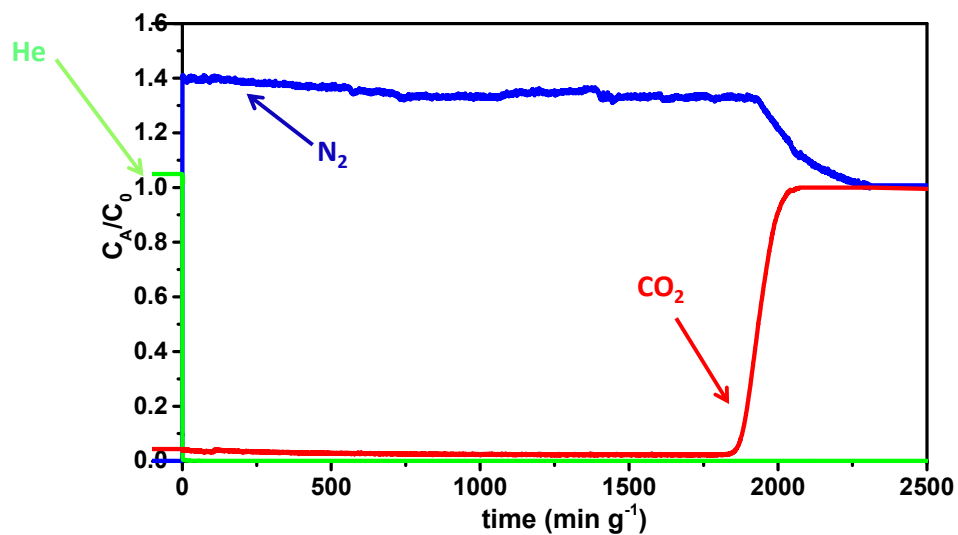


Figure S9. Column breakthrough experiment for **NbOFFIVE-1-Ni** with 1000 ppm CO₂/balance N₂ at 298 K. Breakthrough time of 1880 min/g corresponds to 7.4 wt % CO₂ uptake.

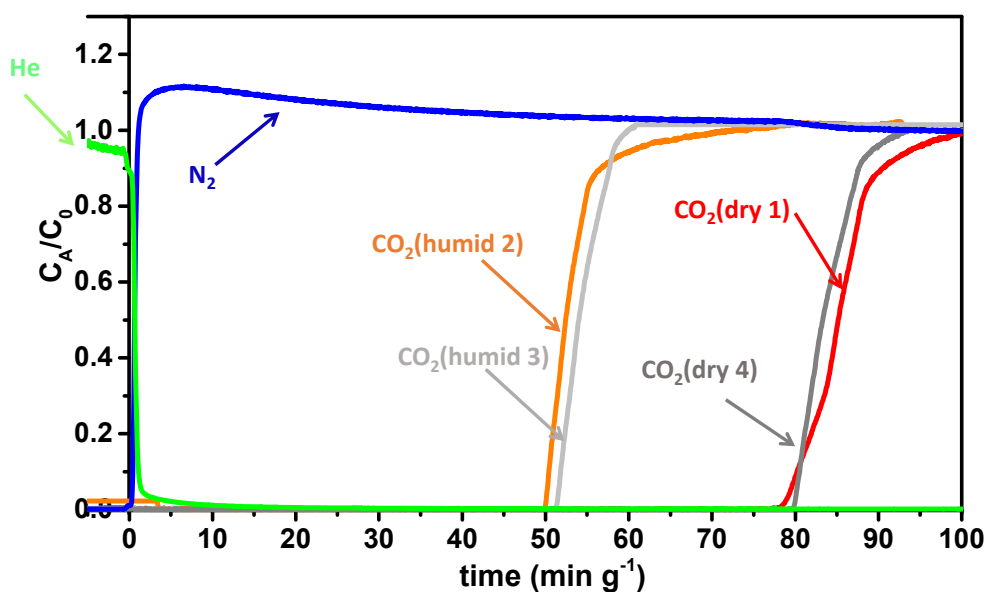


Figure S10. Multiple cyclic column breakthrough tests for the **NbOFFIVE-1-Ni** with the mixed-gas CO₂/N₂ (1%/99%) at 1 bar and 298 K in both dry and humid conditions (50 cm³/min flow rate). Reproducibility of the retention time before (CO₂ dry 1) and after (CO₂ dry 4) humid breakthrough experiments (CO₂ humid 2 and 3) further establishes the hydrolytic stability of the material.

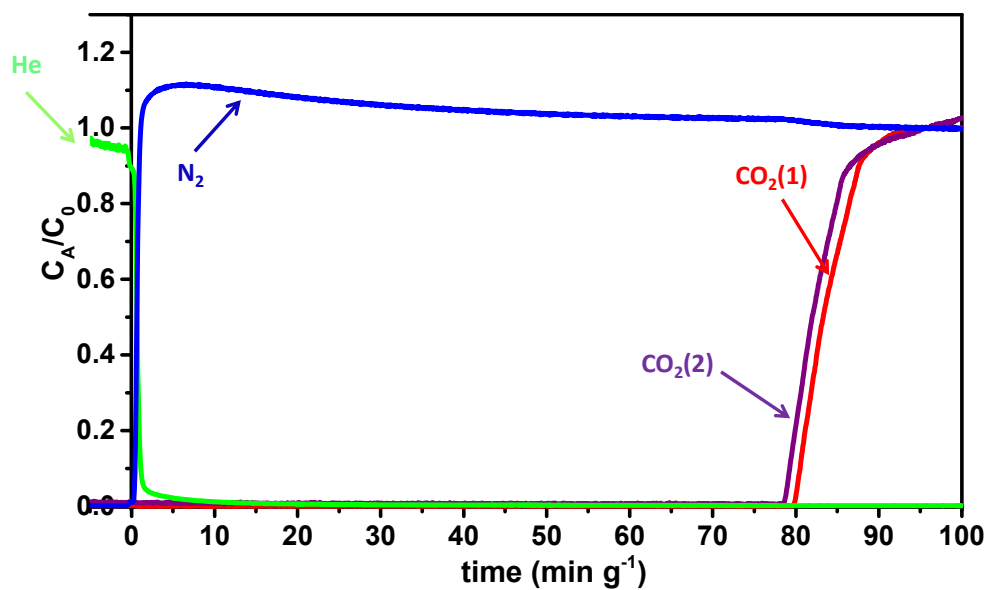


Figure S11. Regeneration under He flow (50 cm³/min flow rate) at 105 °C for 1 hour results in full recovery of the **NbOFFIVE-1-Ni** performance as evident from column breakthrough tests with the mixed-gas CO₂/N₂ (1%/99%) at 1 bar and 298 K (50 cm³/min flow rate) after usual activation (CO₂ (1), 105 °C, vacuum, 6 hours) and after quick activation (CO₂ (2), 105 °C, He flow, 1 hour).

8. TG-DSC experiments

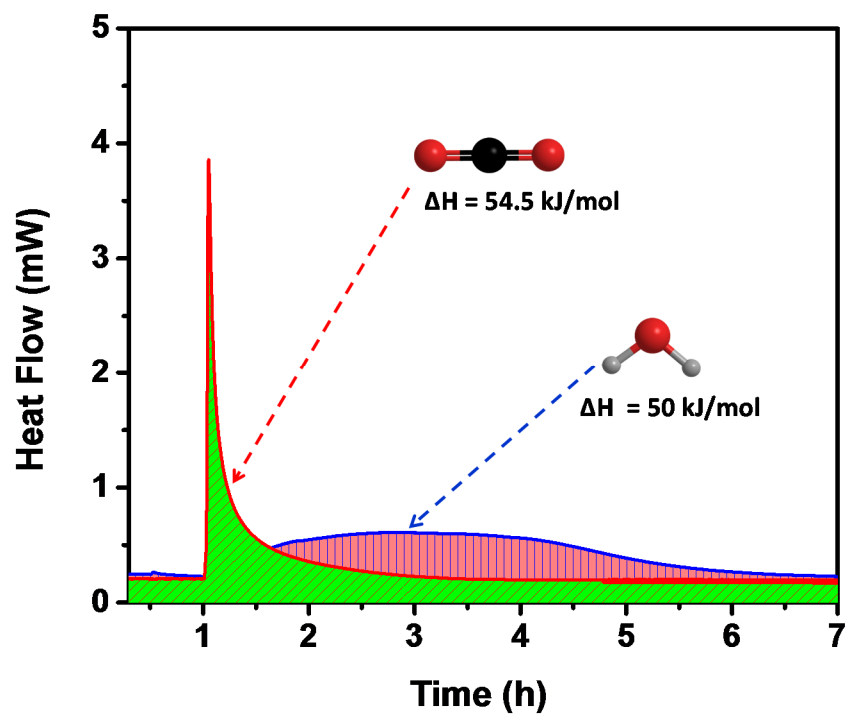


Figure S12. TG-DSC experiments of NbOFFIVE-1-Ni with CO_2 and H_2O at 298 K to determine heat of absorption and uptake simultaneously.

9. References

1. APEX2 (Bruker AXS Inc, Madison, Wisconsin, USA, 2014).
2. SAINT (Bruker AXS. Inc, Madison, Wisconsin, USA, 2014).
3. SADABS (University of Gottingen, Germany, 2008).
4. Farrugia, L. WinGX suite for small-molecule single-crystal crystallography, *J. Appl. Cryst.*, 32, 837-838, (1999); SHELXL-97 (1997); Sheldrick, G. M. Phase annealing in SHELX-90 - direct methods for larger structures, *Acta Cryst. A*, 46, 467-473, (1990).
5. Le Bail, A. *Powder Diff.* 2005, 20, 316.